

## **ZEOLITE-ENCAPSULATED UV-FILTERS: THE KEY FOR MORE SAFE, EFFECTIVE AND ECOFRIENDLY SUNSCREENS**

RICCARDO FANTINI

Dipartimento di Chimica e Scienze Geologiche, Università di Modena e Reggio Emilia, Via G. Campi 103, 41125 Modena

### INTRODUCTION

Solar exposure to UVA and UVB radiation is the main cause of skin cancers, whose incidence is nowadays increasing. Thus, the use, empowerment, and research of new sunscreen products containing UV filters is a fundamental topic for the future of material and life sciences. Sunscreen formulations are the main method of health protection against solar exposure, targeting protection against sunburns, skin aging, skin sensitization, and skin carcinogenesis.

UV filters (UVfs) are organic or inorganic compounds that block UV radiation by scattering, reflecting, or, more often, absorbing UV photons. Most UVfs have limited absorption ranges, and, for these reasons, several filters are combined to obtain broad-spectrum UV protection. Ideally, a UV filter should be photostable and convert the absorbed light into heat, or other forms of energy. Regarding organic UV filters, the absorbed energy is dissipated through three main relaxation processes: i) the emission of new photons (radiative decay, *i.e.* fluorescence and phosphorescence); ii) heat transfer via collisions with surrounding molecules (non-radiative decay); iii) photoisomerization and photodegradation (photochemical reaction). Concerning the latter of these relaxation paths, if the molecule is photoreactive, it can degrade in other entities of unknown toxicity to human health and the environment. UV filters' stability, and consequently safety, strongly depends on the chemical environment, and particularly on the interaction with other components of sunscreens. As an example, the interaction between different UVfs may promote their degradation due to reactions at the excited state. Indeed, sunscreen formulations are complex mixtures, with UVfs representing 2-20 wt.% (Huang *et al.*, 2021). Since many issues are still open regarding their efficacy and stability, much effort has been invested in developing more effective and safe sunscreens. To obtain safer formulations, attempts are made to either obtain new UVfs or to modify the existing UVfs to improve their properties. Stabilizers (*e.g.* single-single (S-S) and triplet-triplet (T-T) quenchers) are typically added to sunscreens to prevent the degradation of UVfs by making more efficient the deactivation process of the UVf's excited states. The encapsulation of organic UVfs is another option to improve their stability.

This work concerns the preparation and characterization of ZEOfilters, which are hybrid UVfs obtained by the encapsulation of the two organic UV filters octinoxate (OMC), and avobenzone (AVO) into zeolites with MOR, FAU, MFI, and LTL framework topologies, and different Si/Al ratio (low-silica: Na-MOR, LTL, ZSM5 30, 13X-FAU; high-silica: HS-MOR, ZSM5-398, HS-FAU). ZEOfilters were deeply characterized by focusing on their composition and properties, and the first results were reported in Fantini *et al.*, 2021.

The project addressed: i) the optimization of ZEOfilters synthesis; ii) the evaluation of their UV filtering performances; iii) the assessment of the efficacy and safety of ZEOfilters in simulated field conditions; iv) the investigation of host-guest and guest-guest interactions.

### MATERIALS AND METHODS

Octinoxate (OMC) and avobenzone (AVO) are two of the most employed organic UVB and UVA filters, respectively, and were purchased from TCI (Tokyo Chemical Industry Co., Ltd.).

AVO (Fig. 1) is a white crystalline powder at room temperature, with melting point at 83.5°C, boiling point at 400-450°C at 1 atm, molecular mass of 310.4 g/mol, and density of 1.221 g/cm<sup>3</sup> (European Chemicals Agency

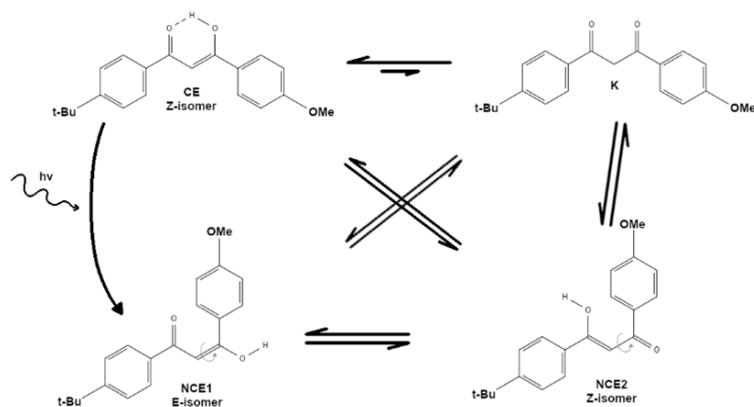


Fig. 1 - Avobenzone conformations: chelated keto-enol (CE), diketo (K), and two non-chelated keto-enol isomers (E-isomer NCE1, Z-isomer NCE2). The bond rotating during CE-NCE1 and CE-NCE2 conversions is shown.

condition, a clear, almost colorless liquid, with melting point at  $-68.3^{\circ}\text{C}$ , boiling point at about  $380\text{-}400^{\circ}\text{C}$ , molecular mass of  $290.40\text{ g/mol}$ , and density of  $1.01\text{ g/cm}^3$  (European Chemicals Agency website (b)). OMC displays its main absorption in the UVB range with a low-energy tail in the UVA interval.

Zeolites are a wide group of mineral and synthetic materials characterized by a crystalline microporous framework. Their channels and cages are usually occupied by  $\text{H}_2\text{O}$  molecules and extra-framework cations but can also host small organic molecules. The chosen framework topologies used in this work are MOR, LTL, FAU, and MFI and are shown in Fig. 3 (plots by VESTA, Momma & Izumi, 2011), while their main features are reported in Table 1.

Concerning the adopted methodologies, pristine synthetic

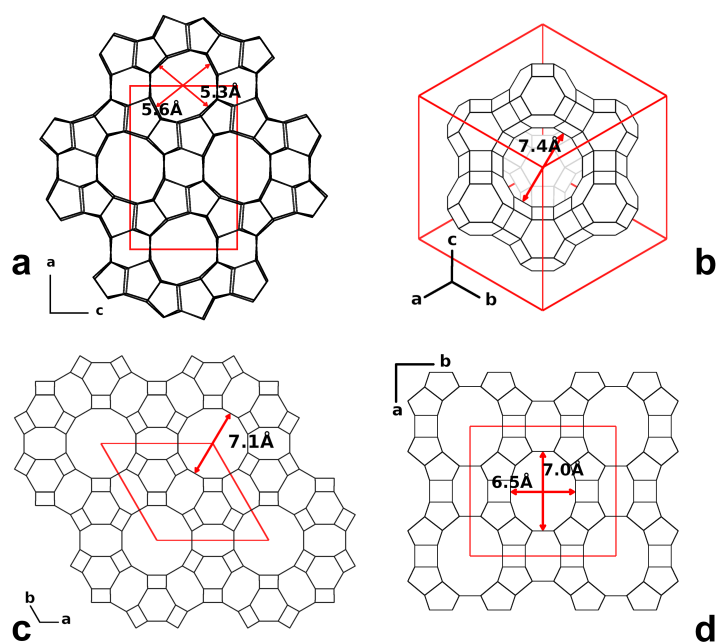


Fig. 3 - Topology of the employed zeolites: a) MFI, b) FAU, c) LTL, d) MOR.

website (a)). AVO displays a large absorption band at  $350\text{-}370\text{ nm}$  with a shoulder at  $380\text{ nm}$  and a weaker band at  $260\text{-}270\text{ nm}$  in different solvents (Biloti *et al.*, 1999; Cantrell & McGarvey, 2001).

OMC (Fig. 2) is used together with other UVfs to reach high SPF values of the final formulations (Antonioni *et al.*, 2008; Vione *et al.*, 2015). During the last decade, OMC has been progressively substituted by other UVfs due to concerns about its potentially harmful effects on the environment. Pure OMC is, at room

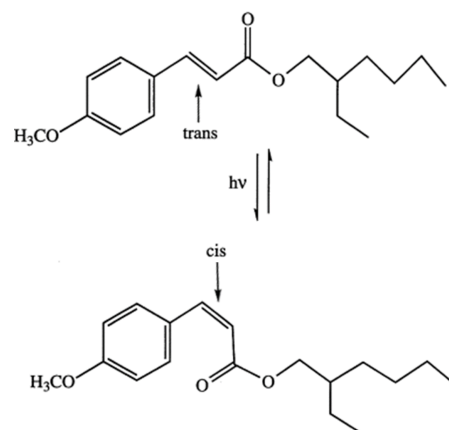


Fig. 2 - Octinoxate trans (E) and cis (Z) isomers.

zeolites were characterized by particle size analysis before UVf loading. A loading procedure of the organic UVfs into different zeolites must be simple, replicable, and must produce a hybrid material with the maximum loading of UVf inside the zeolite and without organic molecules on the zeolite grains surface. The employed procedure can be pointed out into four main steps: i) Zeolite dehydration; ii) Zeolite loading with UVfs; iii) Washing of the hybrid with organic solvent; iv) Hybrid drying. The obtained ZEOfilters were then characterized from a compositional and structural point of view, using: Elemental Analysis (EA); Thermogravimetric Analysis (TGA); Fourier Transform Infrared Spectroscopy (FT-IR);

and Synchrotron-Radiation X-Ray Powder Diffraction (SR-XRPD). Moreover, the performances, efficacy, and stability of ZEOfilters under UV exposure were preliminarily evaluated by: UV-Visible Spectroscopy (UV-Vis); Solar radiation exposure test using a solar lamp; Development of a formulation for the delivery of ZEOfilters; In vitro permeation tests with a Franz cell and Leaching tests of ZEOfilters into simulated seawater.

Table 1 - Features of employed synthetic zeolites. Informal labels, framework topology code, Si/Al molar ratio, chemical formula, space group and unit cell parameters - references in brackets: (1) Fantini *et al.*, 2020; (2) Tanaka *et al.*, 2020, (3) Gigli *et al.*, 2014, (4) Braschi *et al.*, 2010, (5) Olson, 1995, (6) Martucci *et al.*, 2015, # G. Cruciani personal communication - average grain size, and channel system (by International Zeolite Association shorthand notation, the number of asterisks indicates one-, two- or three-dimensional channel systems) (Baerlocher *et al.*, 2007). Si/Al ratios and chemical formulas are from X-ray fluorescence analysis, the grain size was measured by laser diffraction particle analysis.

Label	Framework topology	Unit cell parameters		Channel system (IZA shorthand notation)	Si/Al Mol. Rat.	Chemical formula	Average grain size	Producer (Product code)
		(s.g. a, b, c, V) [Å, Å, Å, Å <sup>3</sup> ]					(Dv 50)	
HS-MOR	MOR	<i>Cmc21</i>	(1)	[001] <b>12</b> 6.5 x 7.0* <<-> [001] <b>8</b> 2.6 x 5.7**	110	~Si <sub>48</sub> O <sub>96</sub>	10 μm	Tosoh Corp. (HSZ-690HOA)
		<i>a</i> 18.0609(2)						
		<i>b</i> 20.2095(2)						
		<i>c</i> 7.4546(1)						
<i>V</i> 2720.9(1)								
Na-MOR	MOR	<i>Cmcm</i>	(2)	[001] <b>12</b> 6.5 x 7.0* <<-> [001] <b>8</b> 2.6 x 5.7**	9.2	Na <sub>5.47</sub> Mg <sub>0.07</sub> (Al <sub>4.97</sub> Si <sub>42.84</sub> )O <sub>96</sub> x 22.7H <sub>2</sub> O	11 μm	Tosoh Corp. (HSZ-642NAA)
		<i>a</i> 18.097						
		<i>b</i> 20.381						
		<i>c</i> 7.493						
<i>V</i> 2763.7								
LTL	LTL	<i>P6/mmm</i>	(3)	[001] <b>12</b> 7.1 x 7.1*	2.9	Na <sub>0.41</sub> K <sub>9.03</sub> (Al <sub>9.14</sub> Si <sub>26.79</sub> )O <sub>72</sub> x 17.1H <sub>2</sub> O	2 μm	Tosoh Corp. (HSZ-500KOA)
		<i>a</i> 18.3795(4)						
		<i>c</i> 7.5281(2)						
		<i>V</i> 2202.4(1)						
HS-FAU	FAU	<i>Fd-3m</i>	(4)	<111> <b>12</b> 7.4 x 7.4***	280	~Si <sub>192</sub> O <sub>384</sub>	38 μm	Tosoh Corp. (HSZ-390HUA)
		<i>a</i> 24.259(4)						
		<i>V</i> 14277.1(4)						
13X-FAU	FAU	<i>Fd-3m</i>	(5)	<111> <b>12</b> 7.4 x 7.4***	1.2	Na <sub>99</sub> Mg <sub>0.3</sub> K <sub>0.2</sub> (Al <sub>86.07</sub> Si <sub>102.40</sub> )O <sub>384</sub> x 236.6H <sub>2</sub> O	5 μm	BDH Chem. Prod. 54017 (out of stock)
		<i>a</i> 25.099(5)						
		<i>V</i> 15811						
ZSM5-398	MFI	<i>P2<sub>1</sub>/n</i>	(6)	{[100] <b>10</b> 5.1 x 5.5 <<-> [010] <b>10</b> 5.3 x 5.6}***	237	Mg <sub>0.22</sub> Ca <sub>0.05</sub> (Al <sub>0.40</sub> Si <sub>95.50</sub> )O <sub>192</sub> x 4.9H <sub>2</sub> O	6 μm	China Catalyst (CCG05Z4001)
		<i>a</i> 19.8999(5)						
		<i>b</i> 20.1174(6)						
		<i>c</i> 13.3892(4)						
		β 90.546(3)°						
<i>V</i> 5359.9(3)								
ZSM5-30	MFI	<i>P2<sub>1</sub>/n</i>	#	{[100] <b>10</b> 5.1 x 5.5 <<-> [010] <b>10</b> 5.3 x 5.6}***	14	H <sub>6</sub> Mg <sub>0.16</sub> (Al <sub>6.40</sub> Si <sub>91.08</sub> )O <sub>192</sub> x 31.8H <sub>2</sub> O	3 μm	China Catalyst (CCG05Z301)
		<i>a</i> 19.9019(3)						
		<i>b</i> 20.1230(3)						
		<i>c</i> 13.3869(2)						
		β 90.501(2)°						
<i>V</i> 5361.1								

## RESULTS AND DISCUSSION

The encapsulation of UV filters octinoxate (OMC) and avobenzone (AVO) into zeolites with MOR, FAU, MFI, and LTL topologies and different Si/Al ratios was tested and discussed.

Different tests were performed by varying the synthesis parameters (temperature, UVf/zeolite ratio, solvent). Finally, a four-step loading procedure was optimized (Fig. 4): 1) zeolite dehydration to remove H<sub>2</sub>O molecules from channels; 2) UVf loading into the zeolite at 100°C to promote molecule diffusivity; 3) ZEOfilter washing with acetone to remove unencapsulated UVf molecules; 4) ZEOfilter drying at 60°C for solvent removal. The final UVf content differs varying zeolite topology, Si/Al ratio, and/or UVf. The optimized ZEOfilters, (*i.e.* without UVf molecule on the external surface of zeolite particles) display a UVf content variable from 13.2% (HS-FAU/OMC) to 1.4% (ZSM5 398/AVO). Particularly, OMC was found to be loaded more evenly in both high- and low-silica zeolites compared to AVO, which is conversely more efficiently trapped in low-silica zeolites compared to their high-silica counterparts (Table 2).

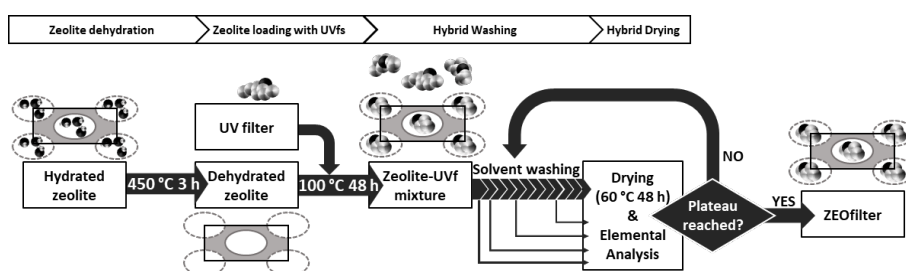


Fig. 4 - Schematic representation of the synthesis procedure of ZEOfilters.

High silica ZEOfilters, generally display a low UV filtering power and appear colored, possibly due to UVf interaction with the zeolite (Fig. 5). The HS-MOR/OMC ZEOfilter was studied by FT-IR to investigate this phenomenon. It was found that the molecule, indeed, undergoes protonation, probably by interacting with the zeolite acid sites. This protonation results in the appearance of visible absorption bands in the UV-vis spectra of the hybrid material (Fig. 6). Among low-silica zeolites, Na-MOR displays no UVf loading, while the protonated ZSM5-30 presents strong absorption colors alike high-silica zeolites. LTL and 13X-FAU are the two more promising zeolites for ZEOfilters production, with LTL slightly overcoming 13X FAU. Indeed, they both display a high UVf content, an enhanced UV filtering power compared to bare UVfs, and almost complete transparency in the visible range (Fig. 6). Thus, LTL and 13X-FAU ZEOfilters were more deeply investigated being the most promising for future applications.

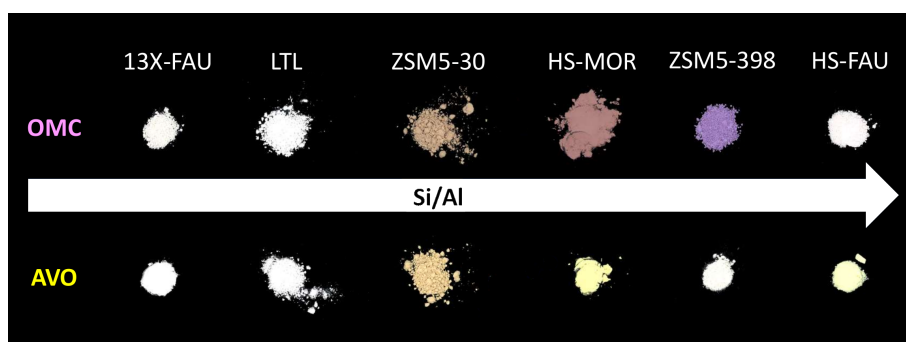


Fig. 5 - Absorption color of ZEOfilters. From left to right Si/Al ratio increases and ZEOfilters show generally darker tones (except for ZSM5-398/AVO and HS-FAU/OMC).

To investigate the interaction between UVfs and the zeolite scaffold, FT-IR experiments were performed on selected samples. FT-IR highlighted a perturbation of the  $\nu(\text{C}=\text{O})$  mode of the OMC carbonyl group when it is encapsulated into HS-MOR and LTL. This kind of perturbation may indicate strong UVf-zeolite interactions, but deeper investigations are ongoing, also aiming at the structural refinement of LTL/OMC ZEOfilter. The major role

of carbonyl groups in the organic-zeolite interaction has been reported in literature. Fois *et al.* (2010) found a carbonyl-K interaction of the fluorenone dye molecule in the L zeolite, also indicating how this interaction is responsible for the fluorenone resistance against H<sub>2</sub>O substitution (Fois *et al.*, 2010).

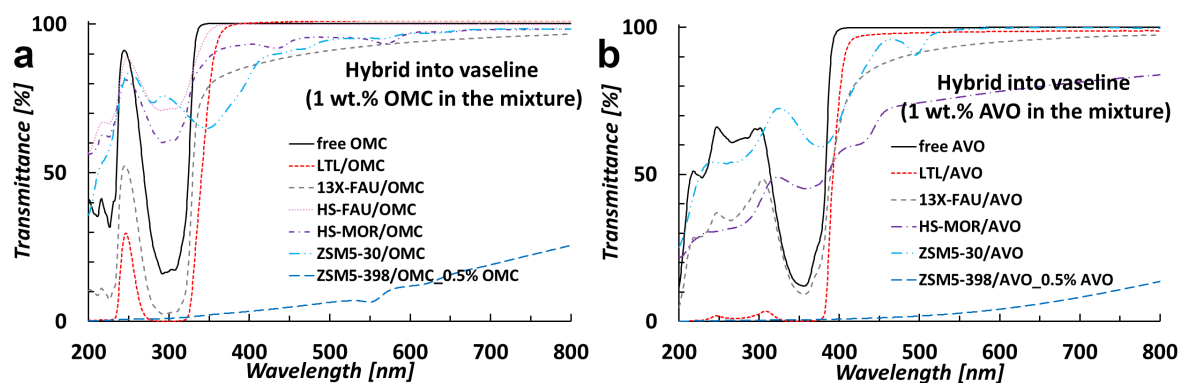


Fig. 6 - UV-Vis spectra of bare UVfs and ZEOfilters in v.o. a) OMC; b) AVO. HS-FAU/AVO is not reported due to the low UVf loading (Table 2).

Table 2 - Overview table of selected ZEOfilters: loading conditions, chemical data from elemental and TG analyses (\* = optimized washing, *i.e.* Total UVf wt.% = UVf wt.% in the zeolite pores). All samples were loaded at 100°C and dried at 60°C before analyses. TGA was not performed on the HS-FAU/AVO, Na-MOR/OMC, and Na-MOR/AVO systems due to the low UV-filter content (na). l/s = liquid/solid ratio during the washing step (zero value indicates a non-washed sample).

Label	Loading conditions		EA		TG		
	UVf/ Zeolite [mol/mol]	l/s [ml/mg]	C [wt.%]	UVf [wt.%]	Total UVf [wt.%]	UVf in the pores [wt.%]	UVf molecules p.u.c. [mol/mol]
13X-FAU/OMC	55.91	0.10	13.53	18.19	16.0	9.9	6.9
		0.16*	4.91	6.60	6.6	6.6	4.3
13X-FAU/AVO	13.20	0.00	17.29	22.34	20.7	16.1	11.2
		0.06*	7.61	9.83	10.6	10.6	6.6
HS-FAU/OMC	87.46	0.60*	10.29	13.83	13.2	13.2	6.1
HS-FAU/AVO	14.88	0.20*	0.46	0.59	na	na	na
Na-MOR/OMC	24.82	4.8*	0.69	0.93	na	na	na
Na-MOR/AVO	1.37	1.07*	0.75	0.97	na	na	na
HS-MOR/OMC	19.96	0.15	8.21	11.03	7.1	7.1	0.8
HS-MOR/AVO	1.30	0.19*	4.60	5.94	4.9	4.9	0.6
LTL/OMC	17.31	0.84	4.17	5.60	5.9	5.3	0.5
LTL/AVO	0.57	0.22*	4.42	5.71	5.3	5.3	0.5
ZSM5-30/OMC	40.31	1.71*	5.87	7.89	7.6	7.6	1.8
ZSM5-30/AVO	5.44	1.55*	3.15	4.07	4.6	4.6	1.0
ZSM5-398/OMC	40.50	1.71*	1.88	2.53	2.6	2.6	0.5
ZSM5-398/AVO	5.83	0.81*	1.09	1.41	1.4	1.4	0.3

Preliminary solar UV exposure tests performed on bare UVfs, and LTL and 13X-FAU ZEOfilters demonstrated high stability of all samples when the compounds were tested independently. In the literature, OMC and AVO are known to degrade under UV exposure in formulations containing both filters, with potentially harmful effects. Unfortunately, exposure tests on mixed ZEOfilters could not be performed during this work. It is expected that formulations containing OMC ZEOfilters and AVO ZEOfilters (simultaneously) should display a high UVf stability since OMC-AVO interactions are inhibited by the zeolite scaffolds.

The use of ZEOfilters in cosmetics should provide several advantages: i) the UVf-skin interaction should be inhibited by the encapsulation; ii) the UVf-UVf interaction should be prevented by the encapsulation of different UVfs separately; iii) the UVf content of formulation may be reduced thanks to their enhanced filtering power; iv) UVf stabilizers and other co-formulants may be reduced thanks to the improved UVf stability. The assessment of UVfs skin permeation is also important for sunscreen safety. Skin permeation tests were preliminarily performed on bare UVfs, and HS-FAU, HS-MOR, LTL, and 13X-FAU ZEOfilters in aqueous suspensions. All systems displayed a very low permeation through the employed pigskin membrane. Preliminary accumulation data of UVfs in the different skin layers demonstrated that most of the UVfs accumulate in the stratum corneum, the outermost skin layer, while a generally very low quantity is detected in the epidermis. The UVf accumulated in the dermis was found to be almost negligible.

During the last decades, UVfs are emerging as a new class of pollutants, especially in the aquatic environment. Leaching tests performed on LTL and 13X-FAU ZEOfilters exhibited very slow and limited leaching of UVfs, but further tests are needed to confirm these results.

## CONCLUSIONS AND FUTURE PERSPECTIVES

Concerning the ZEOfilter optimization, the zeolite particle size will be optimized to improve its stabilization into formulations and consequently the final filtering efficacy. Moreover, the particle size can be optimized for the exploitation of ZEOfilters in products different from cosmetics, *e.g.* plastics and dyes. UVfs are indeed employed also in packaging, where ZEOfilters should also contribute to the product rheology and performance. Also, the synthesis process will be possibly further optimized in view of a possible future scale-up. The UVf amount will be reduced to a minimum so to reduce the employment of organic solvents for the washing of the material. The recovery of UVf from the washing process is also possible, to reduce waste. Moreover, all the working temperatures (*e.g.* zeolite dehydration, filter loading, and final drying) will be lowered as much as possible.

Concerning the exploitability of ZEOfilters, many tests deserve to be performed before their use in cosmetics is launched. Particularly, deeper dermatological and toxicological studies must be performed. The stability of ZEOfilters under UV exposure would also be evaluated with *in operando* UV-Vis and FT-IR measurements, possibly verifying the production of reactive oxygen species and other undesired decay products.

Certainly, the development of such a broad project will require the engagement of industrial partners, bringing expertise, and sharing ideas.

## REFERENCES

- Antoniou, C., Kosmadaki, M.G., Stratigos, A.J., Katsambas, A.D. (2008): Sunscreens-what's important to know. *J. Eur. Acad. Dermatol.*, **22**, 1110-9.
- Baerlocher, C., McCusker, L.B., Olson, D.H. (2007): Atlas of zeolite framework types – Sixth revised edition. Elsevier, Amsterdam, 404 p.
- Biloti, D.N., Dos Reis, M.M., Ferreira, M.M.C., Pessine, F.B.T. (1999): Photochemical behavior under UVA radiation of  $\beta$ -cyclodextrin included Parsol® 1789 with a chemometric approach. *J. Mol. Struct.*, **480**, 557-61.
- Braschi, I., Blasioli, S., Gigli, L., Gessa, C., Alberti, A., Martucci, A. (2010): Removal of sulfonamide antibiotics from water: Evidence of adsorption into an organophilic zeolite Y by its structural modifications. *J. Hazard. Mater.*, **178**, 218-25.
- Cantrell, A. & McGarvey, D.J. (2001): Photochemical studies of 4-tert-butyl-4'-methoxydibenzoylmethane (BM-DBM). *J. Photochem. Photobiol. B*, **64**, 117-22.

- European Chemicals Agency (a): <https://echa.europa.eu/it/brief-profile/-/briefprofile/100.067.779>.
- European Chemicals Agency (b): <https://echa.europa.eu/it/registration-dossier/-/registered-dossier/15876/4/3>.
- Fantini, R., Arletti, R., Quartieri, S., Fabbiani, M., Morandi, S., Martra, G., Di Renzo, F., Vezzalini, G. (2020): Thermal behavior of high silica mordenite. *Micropor. Mesopor. Mat.*, **294**, 109882.
- Fantini, R., Vezzalini, G., Zambon, A., Ferrari, E., Di Renzo, F., Fabbiani, M., Arletti, R. (2021): Boosting sunscreen stability: New hybrid materials from UV filters encapsulation. *Micropor. Mesopor. Mat.*, **328**, 111478.
- Fois, E., Tabacchi, G., Calzaferri, G. (2010): Interactions, Behavior, And Stability of Fluorenone inside Zeolite Nanochannels. *J. Phys. Chem. C*, **114**, 10572-10579.
- Gigli, L., Arletti, R., Tabacchi, G., Fois, E., Vitillo, J., Martra, G., Agostini, G., Quartieri, S., Vezzalini, G. (2014): Close-Packed Dye Molecules in Zeolite Channels Self-Assemble into Supramolecular Nanoladders. *J. Phys. Chem. C*, **118**, 15732-15743.
- Huang, Y., Law, J.C.-F., Lam, T.-K., Leung, K.S.-Y. (2021): Risks of organic UV filters: A review of environmental and human health concern studies. *Sci. Total. Environ.*, **755**, 142486.
- Martucci, A., Rodeghero, E., Pasti, L., Bosi, V., Cruciani, G. (2015): Adsorption of 1,2-dichloroethane on ZSM-5 and desorption dynamics by in situ synchrotron powder X-ray diffraction. *Micropor. Mesopor. Mat.*, **215**, 175-82.
- Momma, K. & Izumi, F. (2011): VESTA 3 for three-dimensional visualization of crystal, volumetric and morphology data. *J. Appl. Crystallogr.*, **44**, 1272-1276.
- Olson, D.H. (1995): The crystal structure of dehydrated NaX. *Zeolites*, **15**, 439-43.
- Tanaka, S., Baba, S., Watanabe, T., Uchida, M. (2020): Preparation and gas permeance of c-axis oriented zeolite membrane using ion-exchanged mordenite zeolite crystals oriented in magnetic field. *J. Eur. Ceram. Soc.*, **40**, 5984-5990.
- Vione, D., Calza, P., Galli, F., Fabbri, D., Santoro, V., Medana, C. (2015): The role of direct photolysis and indirect photochemistry in the environmental fate of ethylhexyl methoxy cinnamate (EHMC) in surface waters. *Sci. Total. Environ.*, **537**, 58-68.